International Journal of Applied Earth Observation and Geoinformation 38 (2015) 25–35

Contents lists available at ScienceDirect

International Journal of Applied Earth Observation and Geoinformation

journal homepage: www.elsevier.com/locate/jag

Semi-automated mapping of burned areas in semi-arid ecosystems using MODIS time-series imagery

Leonardo A. Hardtke[a,*], Paula D. Blanco[a], Héctor F.del Valle[a], Graciela I. Metternicht[b], Walter F. Sione[c,d]

[a] National Patagonian Center-Argentinean National Research Council, Terrestrial Ecology Unit, U9120ACD Puerto Madryn, Chubut, Argentina
[b] Institute of Environmental Studies, School of Biological, Earth and Environmental Sciences, University of New South Wales, Sydney NSW 2052, Australia
[c] Autonomous University of Entre Ríos, CP 3100 Paraná, Entre Ríos, Argentina
[d] UnLu-PRODITEL, 6700 Lujan, Buenos Aires, Argentina

ARTICLE INFO

Article history:
Received 30 September 2014
Received in revised form
18 November 2014
Accepted 21 November 2014
Available online 16 December 2014

Keywords:
Bushfires
Burned area
Time series
Image segmentation
MODIS
Normalized burn ratio
Rangelands

ABSTRACT

Understanding spatial and temporal patterns of burned areas at regional scales, provides a long-term perspective of fire processes and its effects on ecosystems and vegetation recovery patterns, and it is a key factor to design prevention and post-fire restoration plans and strategies. Remote sensing has become the most widely used tool to detect fire affected areas over large tracts of land (e.g., ecosystem, regional and global levels). Standard satellite burned area and active fire products derived from the 500-m Moderate Resolution Imaging Spectroradiometer (MODIS) and the Satellite Pour l'Observation de la Terre (SPOT) are available to this end. However, prior research caution on the use of these global-scale products for regional and sub-regional applications. Consequently, we propose a novel semi-automated algorithm for identification and mapping of burned areas at regional scale. The semi-arid Monte shrublands, a biome covering 240,000 km^2 in the western part of Argentina, and exposed to seasonal bushfires was selected as the test area. The algorithm uses a set of the normalized burned ratio index products derived from MODIS time series; using a two-phased cycle, it firstly detects potentially burned pixels while keeping a low commission error (false detection of burned areas), and subsequently labels them as seed patches. Region growing image segmentation algorithms are applied to the seed patches in the second-phase, to define the perimeter of fire affected areas while decreasing omission errors (missing real burned areas). Independently-derived Landsat ETM+ burned-area reference data was used for validation purposes. Additionally, the performance of the adaptive algorithm was assessed against standard global fire products derived from MODIS Aqua and Terra satellites, total burned area (MCD45A1), the active fire algorithm (MOD14); and the L3JRC SPOT VEGETATION 1 km GLOBCARBON products. The correlation between the size of burned areas detected by the global fire products and independently-derived Landsat reference data ranged from $R^2 = 0.01–0.28$, while our algorithm performed showed a stronger correlation coefficient ($R^2 = 0.96$). Our findings confirm prior research calling for caution when using the global fire products locally or regionally.

Introduction

Over the past few decades wildfires have received significant attention because of the wide range of ecological, economic, social, and political values at stake. Their impacts rely heavily on the intensity, frequency and spatial distribution, which in turn are influenced in complex ways by several natural and anthropic factors (Archibald et al., 2008; Flannigan et al., 2009; Keeley et al. 2008). The understanding of these feedbacks at regional scale depends on an accurate knowledge of the timing and extent of fire events. As collecting fire data in the field is time consuming, expensive and difficult, especially in remote areas, many studies have investigated the ability of satellite imagery to monitor biomass burning and produce accurate burned area estimates, proving to be a cost effective, objective and time-saving tool (Rollins et al., 2004; Chuvieco and Kasischke, 2007; Roy et al., 2005).

Current methods for remote sensing-based mapping and monitoring of wildfires include manual digitalization of burned areas; active fire detection at the time of satellite overpass; threshold-based methods using multi-spectral bands or spectral indices

* Corresponding author. Tel.: +54 280154650252.
E-mail address: hardtke@cenpat-conicet.gob.ar (L.A. Hardtke).

http://dx.doi.org/10.1016/j.jag.2014.11.011
0303-2434/

Table 1
Examples of current methods and techniques for mapping and monitoring wildfires.

Method	Study region	Sensor/Satellite	Reference
Digitalization of burned areas	Sub-Saharan Africa	Landsat ETM+	Silva et al. (2005)
Near real time active fire detection	Global	MODIS	Giglio et al. (2006)
Image thresholding	Amazonia	MODIS	Libonati et al. (2010)
	Spain	MODIS	Quintano et al. (2011)
Spectral indices	Iberian Peninsula	MODIS	Martín et al. (2006)
	North America/Siberia	MODIS	Loboda et al. (2007)
	Boreal fores	NOAA-AVHR	Chuvieco et al. (2008)
Change detection	Global	MODIS	Roy et al. (2005)
	Africa	MODIS	Roy et al. (2002)
Bayesian decision trees	Greece	Landsat TM	Bruzzone and Prieto, (2002)
Classification trees	Sub-Saharan Africa	SPOT-VEGETATION	Silva et al. (2005)
Spectral unmixing	Portugal	NOAA-AVHRR	
Artificial neural networks	Spain	MODIS	Gómez and Martín, 2011
Classification (object oriented)	Thasos Island	Landsat TM	Mitri and Gitas, 2002
Spatial autocorrelation analysis	Italy	MODIS/ASTER	Lanorte et al. (2011)
Regression analysis	Spain	NOAA-AVHRR	Fernandez et al. (1997)
Principal component analysis	Spain	Landsat TM	Siljeström and Moreno-Lopez, 1995
Image segmentation	Spain	SAC-C/MMRS	Garcia and Chuvieco, 2004
Fire radiative power estimation	Northern Australia	MODIS	Maier et al. (2013)
Image thresholding	Australia	MODIS	Maier, 2010
Fire radiative power estimation	NSW and Victoria, Australia	MODIS	Williamson et al. (2013)

Table 2
Selected global fire products assessed for performance in detecting burned areas at regional and sub-regional scale.

Satellite and sensor	Product	Resolution (temporal and spatial)	Period	Tiles	Server download
Terra/Aqua MODIS	MCD45A1 burned area	30 days, 500 m	2001.01.01 to 20011.12.31	h12v12, h12v13, h13v12, h13v13	ftp://ba1.geog.umd.edu/
Terra/Aqua MODIS	MOD14A1 active fire products	8-days summary; 1 km	2001.01.01 to 2011.12.31	h12v12, h12v13, h13v12, h13v13	ftp://e4ftl01u.ecs.nasa.gov/
SPOT VEGETATION	L3JRC	Daily; 1 km	2001.01.01 to 2007.12.31	–	http://bioval.jrc.ec.europa.eu/products/burnt_areas_L3JRC/GlobalBurntAreas2000-2007.php

such as the normalized difference vegetation index (NDVI), the soil-adjusted vegetation index (SAVI), the global environmental monitoring index (GEMI), and the normalized burned ratio (NBR); supervised/unsupervised image classification, logistic regression, principal component analysis and image segmentation, as shown in Table 1.

A range of multi annual global-satellite-derived fire products have been developed over the last decade using automated and semi-automated algorithms for systematic fire-affected area mapping over long time series (Roy et al., 2005; Tansey et al., 2008a; Justice et al., 2002). Some of the most widely used include the SPOT VEGETATION-based global burned area 2000 product, the

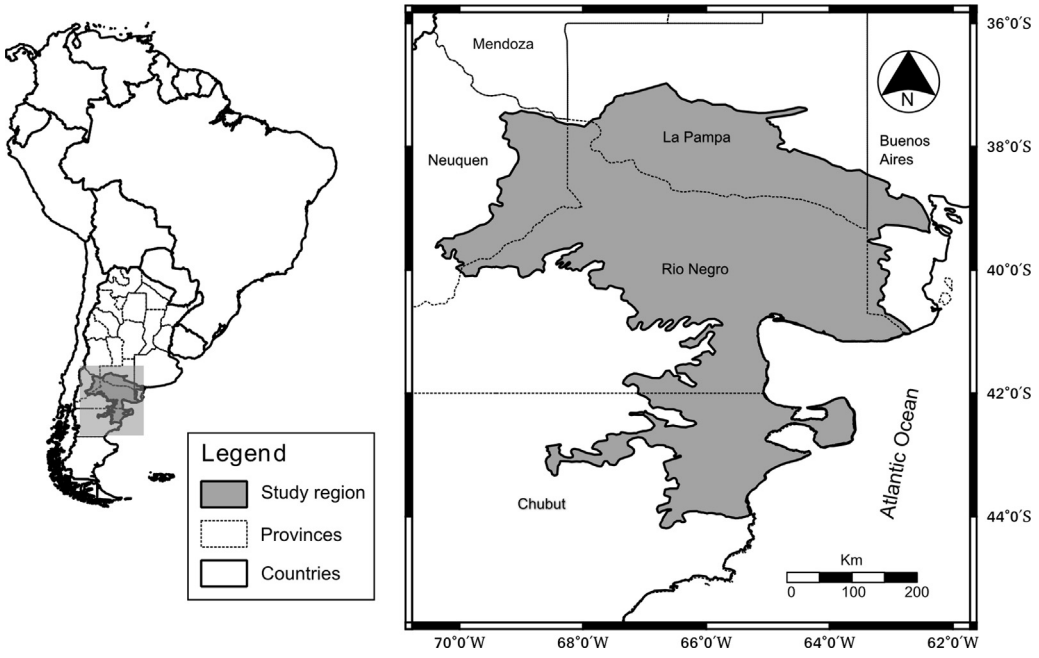

Fig. 1. Location of the pilot study area.

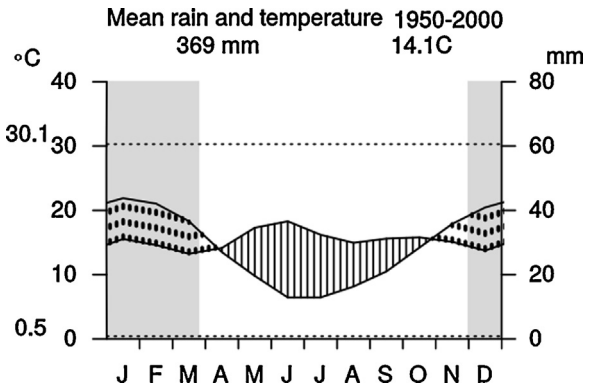

Fig 2. Vegetation types in the study area. (A) Active fire on herbaceous vegetation; (B) Post-fire (previous season wildfire) vegetation recovery; (C) Post-fire (fourth previous season wildfire) vegetation recovery; (D) Sheep grazing degraded area, showing isolates herbaceous an shrub patches.; (E) Area covered by low shrubs and herbaceous; (F) Vegetation in a single shrub layer of Chuquiraga avellanedae; (G) Area of dense herbaceous vegetation; (H) Area dominated by shrubby vegetation. mainly Larrea divaricata; (I) Area of mixed shrubby vegetation.

GBA 2000 (Grégoire et al., 2003) and GLOBSCAR (Simon et al., 2004), the Leicester, Louvain-la-Neuve, Lisbon and JRC terrestrial ecosystem monitoring global burnt area product (better known as L3JRC) (Tansey et al., 2008a), and the MODIS-derived burned area (MCD45A1) (Roy et al., 2005; Giglio et al., 2009), and active fire detection (MOD14) products (Tansey et al., 2008a). While these fire products appear suitable at the global scale, detection and mapping of burned areas at regional and local levels remains challenging due to the diverse and complex patterns associated to the spectral response of burned areas over space and time. For instance, Loboda et al. (2007) showed that global fire products efficiency may vary in different ecosystems, while Tansey et al. (2008b) indicated the agreement between the MODIS active fire and burned areas products are spatially variable and dependent on vegetation type and function, revealing discrepancies in areal estimates, timing, and location of fire affected areas. These authors also highlighted the need for systematic product validation; moreover, Roy and Boschetti (2009) cautioned that global fire products may not meet the accuracy requirements needed for regional and local scale studies.

The aforementioned research indicates a knowledge gap in the reliability of global fire products to deliver value added information on wildfires extent and impacts at regional and local scales. Accordingly, this paper investigates whether global fire products can cater for the provision of accurate data and information on wildfires (or bushfires) over small areas, and/or complex spatial patterns that are common to semiarid ecosystems. To this end we developed and tested a novel algorithm for automatic delimitation of burned areas at regional or local scale, using the semi-arid Monte ecosystems of Argentina as pilot study area, and compared its performance with selected MODIS-and SPOT VEGETATION-derived global fire products. Materials and methods Section describes the pilot study area and remote sensing data acquisition, while Method Section presents the methodological framework adopted for the implementation of the algorithm, the development of an independent data set for validation of the outputs, and the assessment of its performance against global fire products. Results and discussion

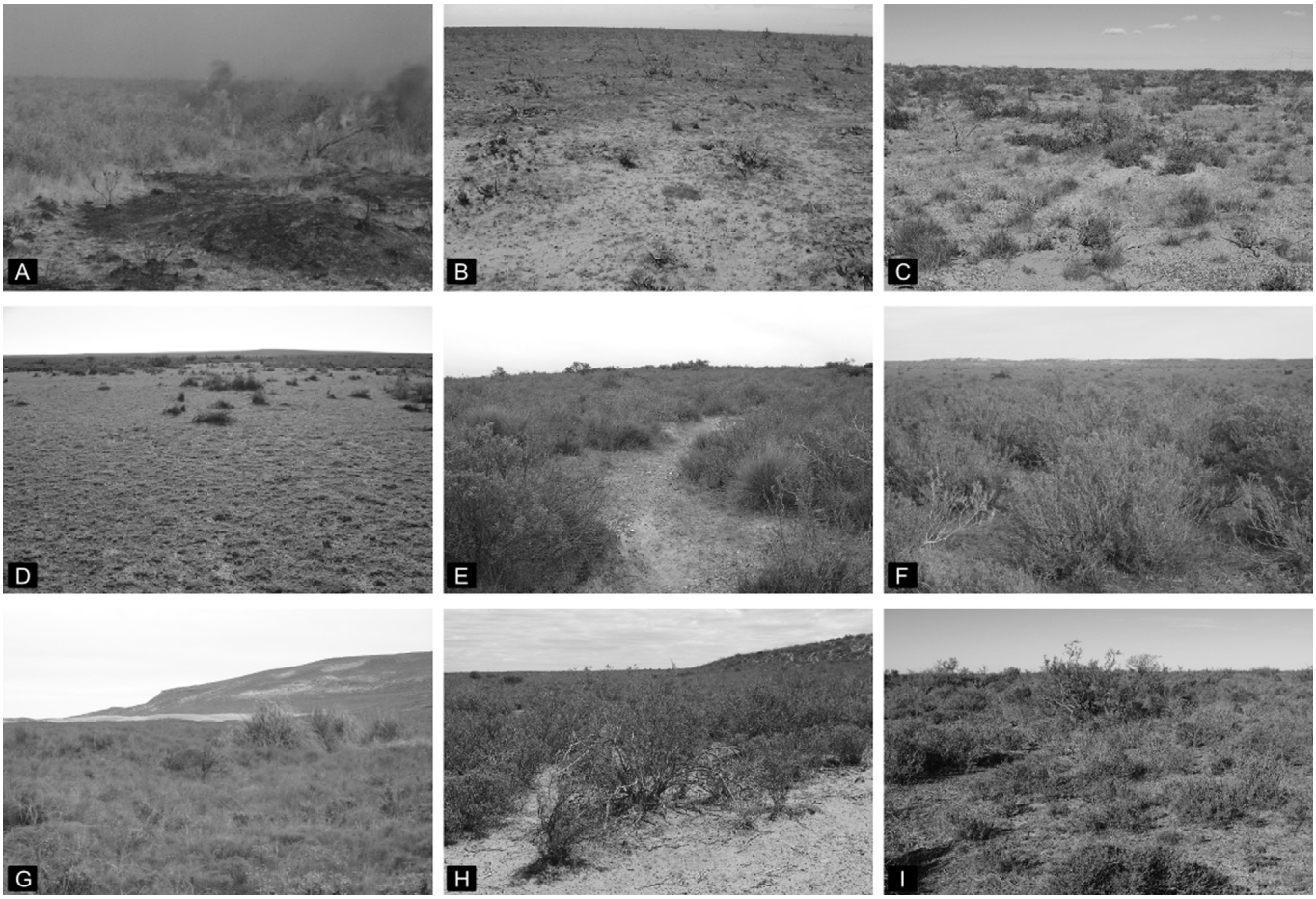

Fig. 3. Climatic diagram for the study area based on temperature and precipitation data of Worldclim (1950–2000), averaged over the full extent of the study area. Shaded areas showing the fire season, stippled areas the drought stress and striped areas the water excess period.

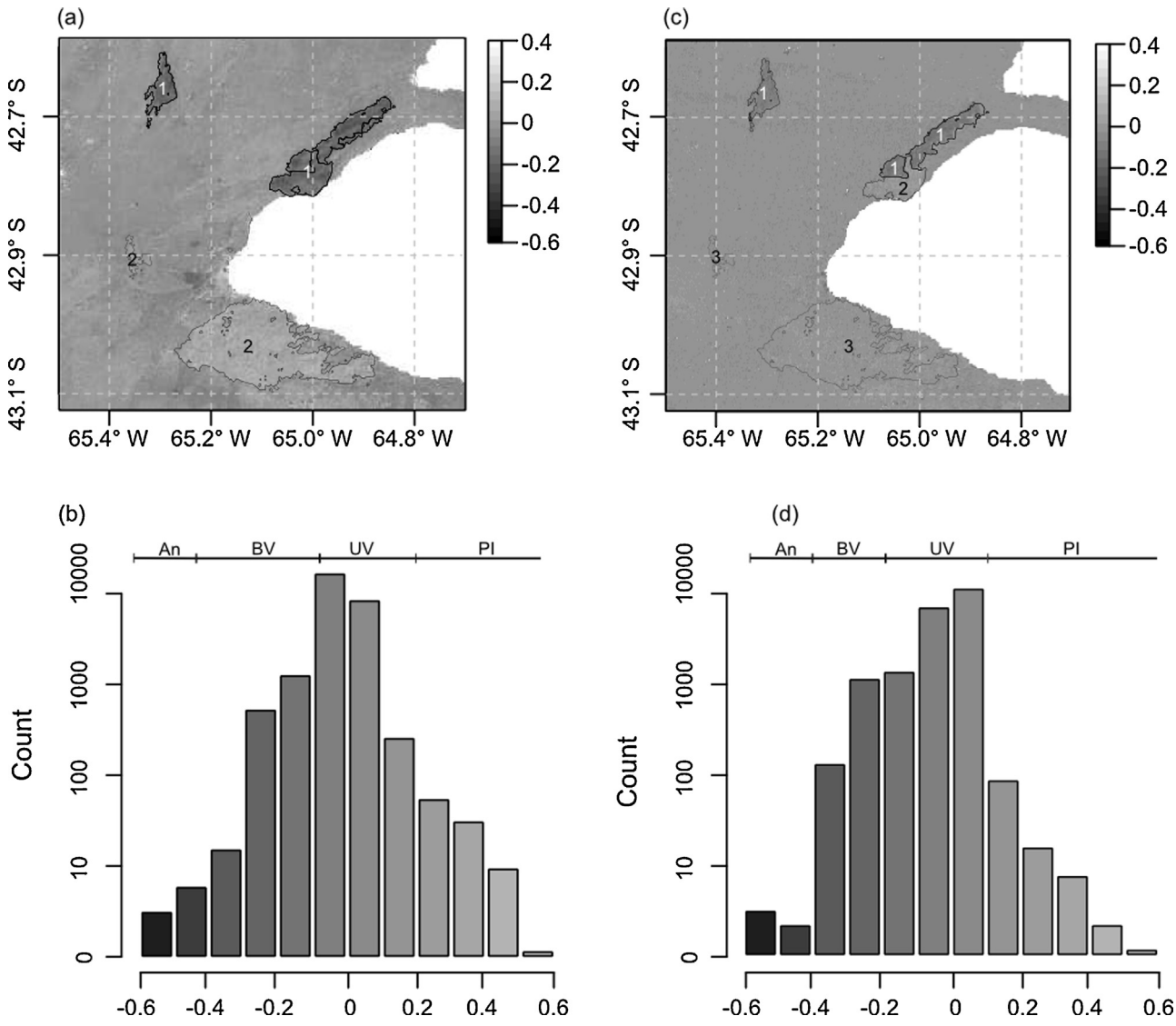

Fig. 4. Maps of normalized burn ratio (NBR) corresponding to Julian day 33, (a) NBR index map showing recently burned areas (1), and previous season burned areas (2); (b) Frequency histogram (logarithmic) of NBR index values [*]; (c) *d*NBR index map showing recently burned areas (1), previous date burned areas (2), and previous season burned areas (3); (d) Frequency histogram (logarithmic) of *d*NBR index values[*]. [*]NBR typical ranges: An – anomalous values; BV – burned vegetation; UV – unburned vegetation; and PI – productivity increase for 2002-003, indicating typical ranges for: An – anomalous values; BV – burned vegetation; UV – unburned vegetation; and PI – productivity increase.

and Conclusion Section discuss the results with emphasis on error sources, and main conclusions and recommendations, respectively.

Material and methods

Pilot study area

The Patagonian Monte biome is a semiarid ecosystem located in western Argentina, extending from 24°35′S to 44°20′S (León et al., 1998) (Fig. 1). Vegetation corresponds to a shrubland with frequent herbaceous strata where vegetation cover rarely exceeds 60% (Fig. 2). The climate is semiarid to arid, with high evaporation enhanced by windy conditions. Western winds predominate all the year round. Mean annual rainfall varies between 150 and 850 mm, while the mean annual temperature varies between 13 and 15 °C (Fig. 3) (Hijmans et al., 2005; Labraga and Villalba, 2009).

Wildfires and domestic grazing are the main disturbance agents in this region (Villagra et al., 2009). There are three historical periods where fire played different roles in the ecological dynamics of the area; in ancient times and up to the end of the 19th century, the indigenous people frequently burned the shrublands for hunting, communication or other purposes (Claraz, 1988). After the introduction of domestic livestock (mainly sheep) at the end of the 19th century and up to the 1980s, dramatic changes occurred in the vegetation dynamics due to grazing disturbance (Ares et al., 1990; Soriano et al., 1983) and frequency fire disruption (Defosse et al., 2003). Increasing grazing pressure since the late 1980s has resulted in relented recovery of grasslands and the consequent accumulation of dead grass biomass, which in turn has increased fire events frequency and magnitude (del Valle et al., 2004). Currently the region lacks a fire management plan; only firewalls are built in peri-urban areas to protect properties.

Input data set and pre-processing

The primary input for the proposed burned area algorithm was the 2000–2011 time series of the MODIS-derived normalized burned ratio index (NBR), and the temporal difference of consecutive images ($d\mathrm{NBR}_t = \mathrm{NBR}_t - \mathrm{NBR}_{t-1}$) described in the next Section.

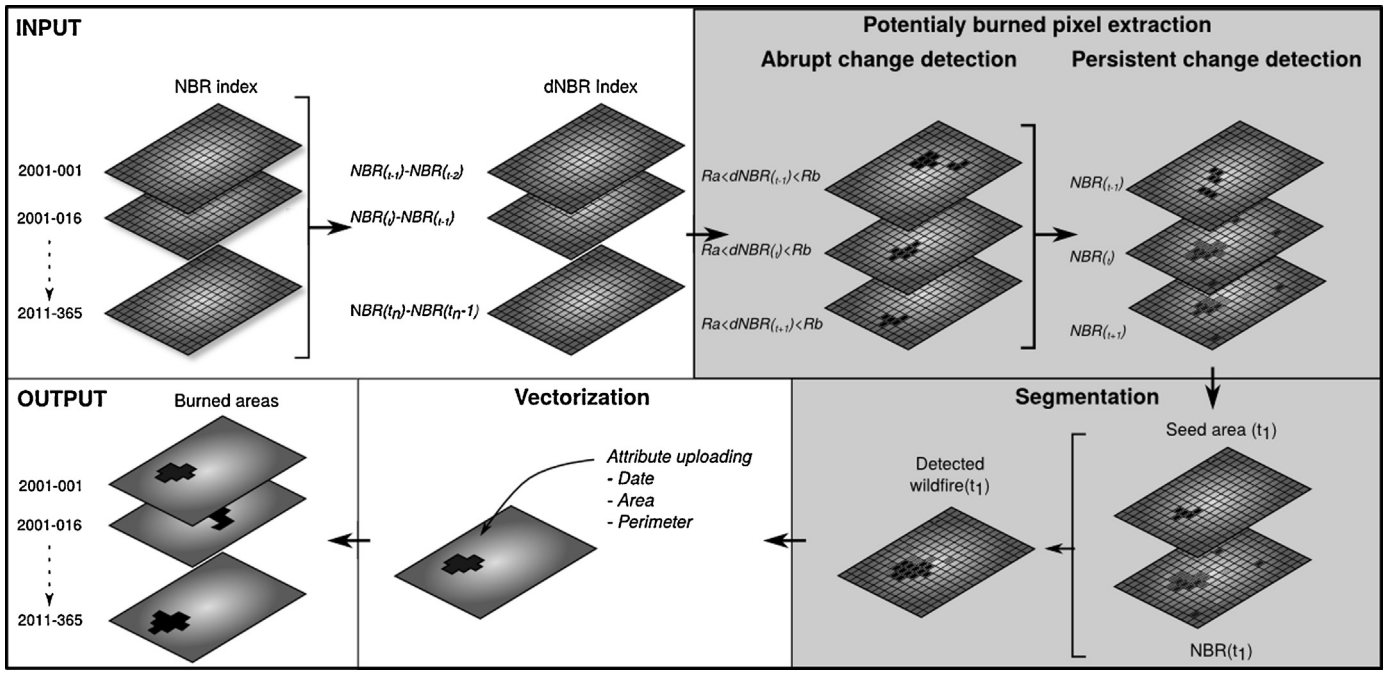

Fig. 5. Workflow of the burned areas detection algorithm indicating input and output data (white panels) and the main processes (Grey panels). The algorithm is applied recursively to each image in the time series, from 2001-001 to 2011-365.

The NBR index serves to detect burned areas, while the *d*NBR measures burn severity. Even though both indices were originally developed for use with data input from Landsat TM/ETM+ sensors imagery (Key and Benson, 1999), they were later successfully adapted to other sensors data (e.g., MODIS) showing spectral band configurations sensitive to fire-related landscape features (Loboda et al., 2007).

The NBR index for the study area was obtained using 16 days composites (maximum value composite) of MODIS surface reflectance product (MOD13Q1), bands 2 (0.841–0.876 μm) and 7 (2.105–2.155 μm) downloaded in hierarchical data format (HDF) and sinusoidal cartographic projection. Key and Benson (2006) equation was applied for the NBR index as follows:

$$\mathrm{NBR} = \frac{(\mathrm{band2} - \mathrm{band7})}{(\mathrm{band2} + \mathrm{band7})} \quad (1)$$

where NBR takes values ranging between −1 and 1; positive values occur over vegetated areas, while negative values correspond to bare surfaces. Burned areas present negative NBR values, depending on burn severity (Escuin et al., 2008).

The temporal difference of two consecutive dates (*d*NBR index) was obtained with the following equation:

$$d\mathrm{NBR} = \mathrm{NBR}_t - \mathrm{NBR}_{t-1} \quad (2)$$

Theoretically, due to the NBR data range, *d*NBR can range between −2 and +2. According to Keeley (2009), typical data values vary between −0.55 to +1.35. Positive $d\mathrm{NBR}_t$ values will result from NBR_t being greater than previous NBR_{t-1}. This may be due to increased plant productivity at time *t* of the NBR image acquisition, thus resulting in $d\mathrm{NBR}_t$ values ranging from 0.10 to 0.50. Clouds or anomalies in the NBR_{t-1} result in *d*NBR values above 0.5. Typical unburned pixels fall approximately in the range near zero of the

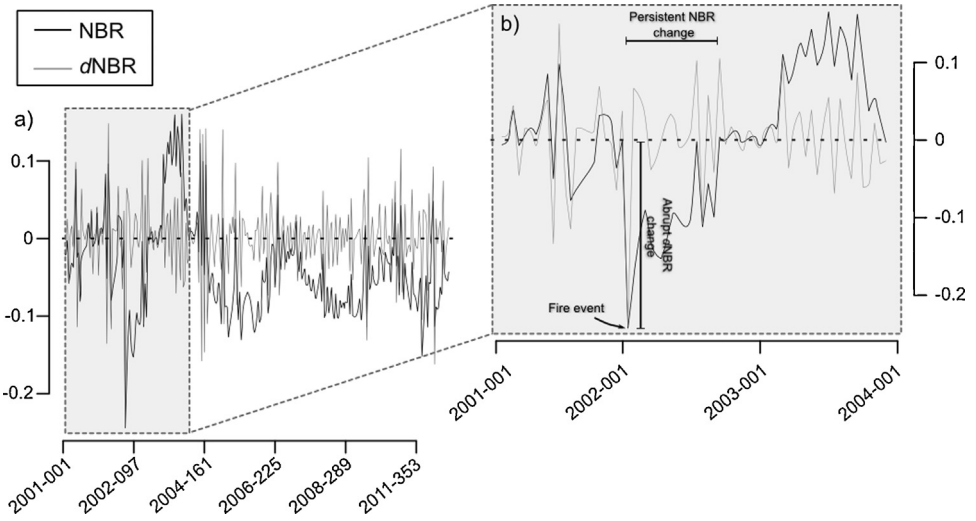

Fig. 6. Temporal variation of the average of the NBR and DNBR index on a burned area, (a) Complete time series (2001-001 to 2011-353); (b) Detail of the 2001-001 to 2004-001 period, indicating the abrupt change in the *d*NBR index and persistent change the NBR index.

*d*NBR index (−0.10 to 0.10), indicating relatively little or no change over the time interval considered. Typically, a burned pixel shows $dNBR_t$ values in the −0.1 to −0.55 range due to a decrease of NBR_t in comparison to NBR_{t-1}, produced by a wildfire. These threshold values, for both NBR and *d*NBR, are consistent with those found in our study area (Fig. 4).

To match the extent of the study area, subsets of four image tiles (h12v12, h12v13, h13v12 and h13v13) were extracted, covering 2655 × 2948 pixels. The images were referenced to the Universal Transverse Mercator Zone 20 South projection, resampled to a pixel size of 250 × 250 m and converted to Geo-tiff format using the GDAL library. This process resulted in 272 index images of NBR and *d*NBR time series for the period 18 February 2000–31 December 2011 (see Fig. 5), each one derived from 16 days composite MODIS images; the index images were incorporated in a geographic database for further analysis.

Lastly, all pixels marked as snow, ice or water bodies in the MODIS composites were masked to avoid false positives in these areas. The pixels labeled as clouds or with marginal quality were removed and replaced by digital numbers derived from a temporal spline interpolation, to avoid extreme values in the temporal series, where data from one scene replace missing data in the other scene.

Method

The burned area algorithm

Fig. 5 shows a flowchart summarizing the methodological steps of burned areas algorithm. The input data are the normalized burned ratio index derived from the MODIS time series aforementioned. The mapping accuracy of the output results was assessed using reference data obtained from independently-derived Landsat Enhanced Thematic Mapper Plus (ETM+) burned-areas, described in the following Section.

Algorithm development

The burned area algorithm works in two phases, executed iteratively. The first phase aims to detect 'potentially burned' pixels while keeping a low commission error (false detection of burned areas); these pixels become 'seed patches' and are input to a region growing image segmentation algorithm to delineate the perimeter of the fire affected area, decreasing omission errors in this process (missing real burned areas).

The first phase of detecting potentially burned areas includes two stages; the first one aims to detect abrupt changes and the second one to detect persistent changes (Fig. 6). Considering the theoretical *d*NBR values described in the previous Section, in the first stage we extracted all pixels with *d*NBR values between −0.1 and −0.55. Spectral changes induced by fires should be persistent overtime; that is, negative NBR values should be consistently observed during a time span after detection of a burned area. That premise guides the second stage, which keeps only pixels from the first stage whose NBR values remains below −0.1 in the following three image dates (e.g., representing a total of 48 days post- burned area detection, given the use of MODIS 16 day composites for the production of the NBR images). The resulting pixels are labeled as seed areas.

The second phase uses the seed patches to define the perimeter of the burned area through applying a region growing image segmentation algorithm. This technique requires a seed area that is considered to be representative of the object (potentially burned

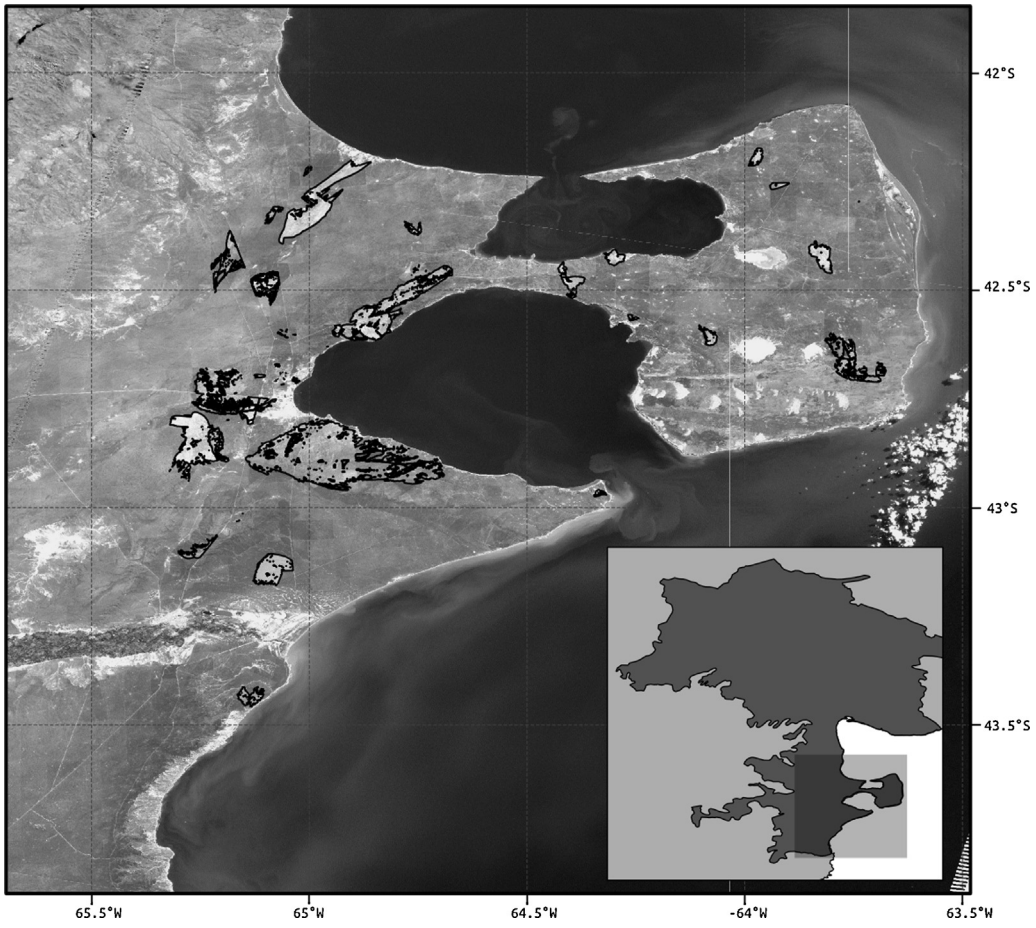

Fig. 7. Landsat TM mosaic of the validation area after the 2011 fire season, showing the reference burned areas of the 2001–2011 period.

area) to be segmented; applying a pre-determined criterion, neighboring pixels are evaluated to determine if they should also be part of the object. If so, they are added to the seed area, and the process continues iteratively until no new pixels are added to the area. Our research used the connected threshold criterion (Pratt, 2001), with an interval of NBR values obtained empirically ($-0.1 < NBR < -0.4$). This algorithm was implemented as an ad hoc function within the r.mapcalc module of GRASS-GIS. Lastly, each individual burned area was vectorized, and an attribute table with a unique identifier was generated specifying the approximated burned date (eg., using the MODIS 16 days composite date as reference) and areal extent of each fire occurrence. The aforementioned process enabled gathering a comprehensive database of burned areas over the Monte ecosystem, for the 2000–2011 period.

Validation with independently-derived reference data

Validation processes require independent reference data sources, which should have a known precision level and cover a representative proportion of the study area. Reference data derived from higher spatial resolution satellite imagery have been used extensively to validate lower spatial resolution burned area products (e.g., Barbosa et al., 1998; Fraser et al., 2000; Boschetti et al., 2006; Tsela et al., 2014). Even though this approach presents some challenges due to potential geometrical displacements (Eva and Lambin, 1998), several authors (Eva and Lambin, 1998; Silva et al., 2005; Roy and Boschetti, 2009) have suggested the comparison of two sources with differing spatial resolution is possible based on the analysis of the proportion of affected area falling within each cell in a large grid, covering the target area.

Reference burned area perimeters were obtained by supervised classification (Fig. 7) of Landsat ET/ETM+ images of 30 m spatial resolution. We analyzed images of the end of the fire season (April or May) for each year between 2001 and 2011 over an area that covered approximately 37,250 km^2, corresponding to 15% of the total area. The area was extracted from four Landsat scenes and referenced to the unique Landsat Worldwide Reference System (WRS-2) path rows 243 89, 243 90, 244 89 and 244 90. These maps were considered the best available reference data and were used for comparison with the burned area maps.

Linear regression equations were fitted between the results generated by the burned areas algorithm applied on the MODIS-derived NBR, and the independently derived Landsat reference estimations of burned area using a 5×5 km grid. The regression coefficients provide a general indication of over- or under- estimation of burned areas. A slope of one indicates that the output products estimate exactly the same extent of burned areas as the reference data; a slope of less than one indicates overestimation, and greater than one is related to underestimation of burned areas.

Comparison with global fire products

Selected global fire products currently available from various satellite sensors, were used for comparing performance in detecting and mapping burned areas at regional and sub-regional scale against the outputs of our algorithm (Table 2). The complete time series for each of the products described in Table 2 were incorporated into a GIS database.

In this work, MCD45A1 burned area and MOD14A1 active fire products, and the SPOT VGT derived L3JRC products were used to compare their performance with the results of our algorithm. For the MODIS 8-day summaries active-fire-data (MOD14A1) all pixels classified as fire-pixels were considered, whatever their confidence level, because false detection sources, like industrial and urban land-cover boundaries, sun-glint around coastlines, and volcanoes (De Klerk, 2008; Giglio et al., 2006) are unlikely in the studied area. For the monthly 500 m burned area product (MCD45A1) we considered all pixels classified as burned, not considering pixels flagged as water, cloud, cloud shadow or snow. The L3JRC product is available as annual composited 1-km gridded data in geographic coordinates, with the Julian day of the first burned-area detection within a fire year. For the L3JRC product, we considered all pixels classified as fire-pixels.

Spatial-temporal attributes of burned areas

The results obtained by applying the algorithm were used to characterize some basic attributes of the burned areas, which are important characteristics to predict vegetation successional pathways and recovery patterns post-fire (Thonicke et al., 2001). We estimated the total burned area, the fire size distribution, fire recurrence and mean fire return interval (FRI), which is the length of time between fires at a specific point on the landscape. The later was calculated following Forsyth and Van Wilgen (1998) equation:

$$FRI = \frac{y}{(b/a)} \quad (3)$$

where FRI is the fire return period in years, b is the area of all fires recorded over y years and a is the area over which fires were recorded.

Results and discussion

The burned area algorithm validation

A total of 1490, 5×5 km grid cells covering the validation area (37,250 km^2) were considered in the validation process. The independently derived reference data indicates that 132 (8.85%) grid-cells were affected by a total of 21 individual wildfires in different proportions. The outputs of the burned area algorithm are in a close agreement with the Landsat reference data; the overall regression slope between our results and the reference burned areas perimeters was 0.99, with R^2 equal to 0.96 (Fig. 8).

Error sources

Detection errors

(a) Omission errors:

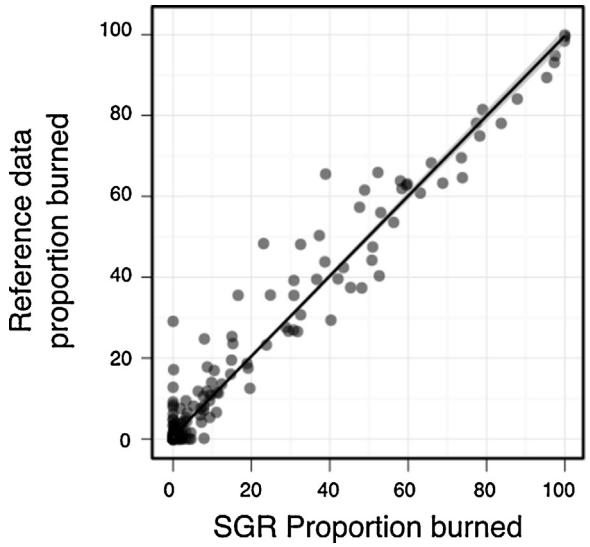

Fig. 8. Scatter plot of the proportions of 5×5 km cells labelled as burned by the burned area algorithm, plotted against the proportion labelled as burned by reference data. Each point is plotted with a gray shade to reflect point's density. The regression line is plotted as a solid black line, and smoothed 0.95 confidence interval in gray. period.

i) Low severity wildfires can produce minimal changes in *d*NBR (Key and Benson, 2006), in fact fires would not be detected if these changes were smaller than the *d*NBR threshold. However, since only pixels with time-persistent NBR changes are chosen as seed pixels in the second phase of the burned area algorithm (see The burned area algorithm Section), relaxed *d*NBR threshold values may be chosen without increasing false detection rate, while keeping low omission errors.

ii) Rapid vegetation recovery in burned areas (regrowth occurring in less than 48 days) would generate non-persistent changes in the MODIS-derived NBR index, so those pixels would fail to be marked as seeds. It is very unlikely to happen in semi-arid Montes of the study area due to its climate and vegetation types. This error type could affect burned area detection in biomes where vegetation regrows quickly after a fire event. In these cases, a reduction of the time span threshold should be evaluated (e.g., from 48 days to 32 days).

iii) Errors in NBR images, due to instrument problems or clouds could result in *d*NBR values outside the typical range (see Input data set and pre-processing Section) which would prevent correct identification of seed areas. Our research shows this type of errors occur in isolated pixels, thus medium-sized burned areas, with several seed pixels should be detected, despite potential errors in the satellite data.

(b) Commission errors:

i) The design of the burned area algorithm determines a low likelihood of commission errors. This type of error would occur if a non-burned pixel shows a marked change in the NBR index value, which should also be time-persistent (e.g., by at least 48 days). In addition to a very unlikely repeated error in MODIS composite images, we do not know another source of such behavior.

Mapping errors

(a) Omission errors:

i) Underestimation of burned areas could happen in areas where fires have not been intensive, causing low severity burned (e.g., areas with low NBR values). Because the burned area algorithm is designed to allow using "relaxed" growth thresholds, this type of error can be controlled and decreased without an increase in commission errors.

Table 3
Accuracy in detection of burned areas at regional scale of global products.

Product	R^2	Intercept	Slope
L3JRC (VGT burned areas)	0.01	6.18	(slope = 0.06)
MOD14A2 (active fires)	0.25	5.09	(slope = 0.97)
MCD45A1 (burned areas)	0.05	7.57	(slope = 1.15)

(b) Commission errors:

i) Overestimation of burned areas could occur if a fire develops adjacent to a previously burned area, provided the areas still show low NBR values (i.e., recently burned, not fully recovered). This phenomenon was not observed in the study area, and if it happens it could easily be solved by a post-processing step in GIS software.

Comparison with global fire product

The global fire products (L3JRC, MOD14A2, MCD45A1, see Table 2) showed a poorer agreement with the reference data in comparison with estimations from the burned area algorithm, as evidenced by the low R^2 values of the fitted regression models (see Table 3 and Fig. 9). The analysis of the slopes of the regression models indicates the largest over-estimation of fire-affected areas to occur when using the SPOT VEGETATION L3JR6 followed by MOD14A2 (active fire). In contrast, the MOD45A1 (burned areas) underestimates moderately the areal extent of burned areas. The intercept of the regression models is relatively high (Table 3), indicating that all the global fire products failed to detect small patches of burned areas. It is worth noting the significant underestimation of burned areas detection by MOD45A1; all the burned areas being lesser than 60% compared to burned area detection by Landsat.

Global fire products have been validated in different regions of the world with contrasting results (Table 4). A comparison between the validation performed in this work and by other authors is useful to detect and describe possible error sources. Tsela et al. (2010) validated MOD45A1 across different biomes in South Africa, and found generally better agreement with reference data, with R^2 ranging between 0.38 and 0.86 and slopes between 0.48 and 0.92 depending on the vegetation type. These differences could be because this validation was performed over a short period (4 months) on a single fire season, and therefore may not have captured the full range of patch sizes and fire behavior.

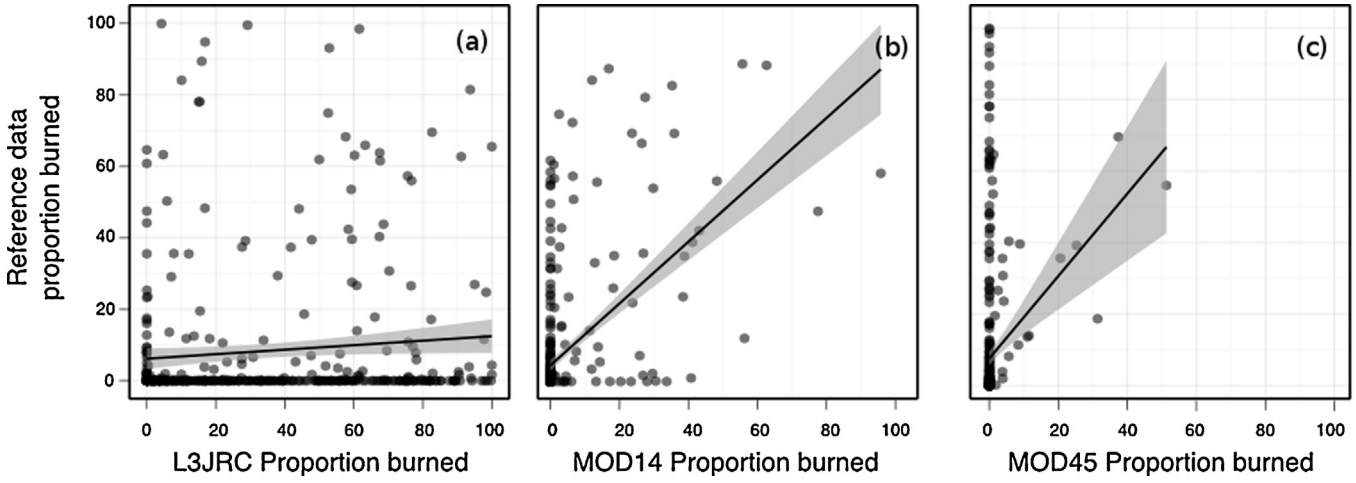

Fig. 9. Scatter plot of the proportions of 5 × 5 km cells labelled as burned by the (a) L3JRC (b) MOD14 (c) MOD45, plotted against the proportion labelled as burned by reference data. Each point is plotted with a gray shade to reflect point's density. The regression line is plotted as a solid black line, and smoothed 0.95 confidence interval in gray.

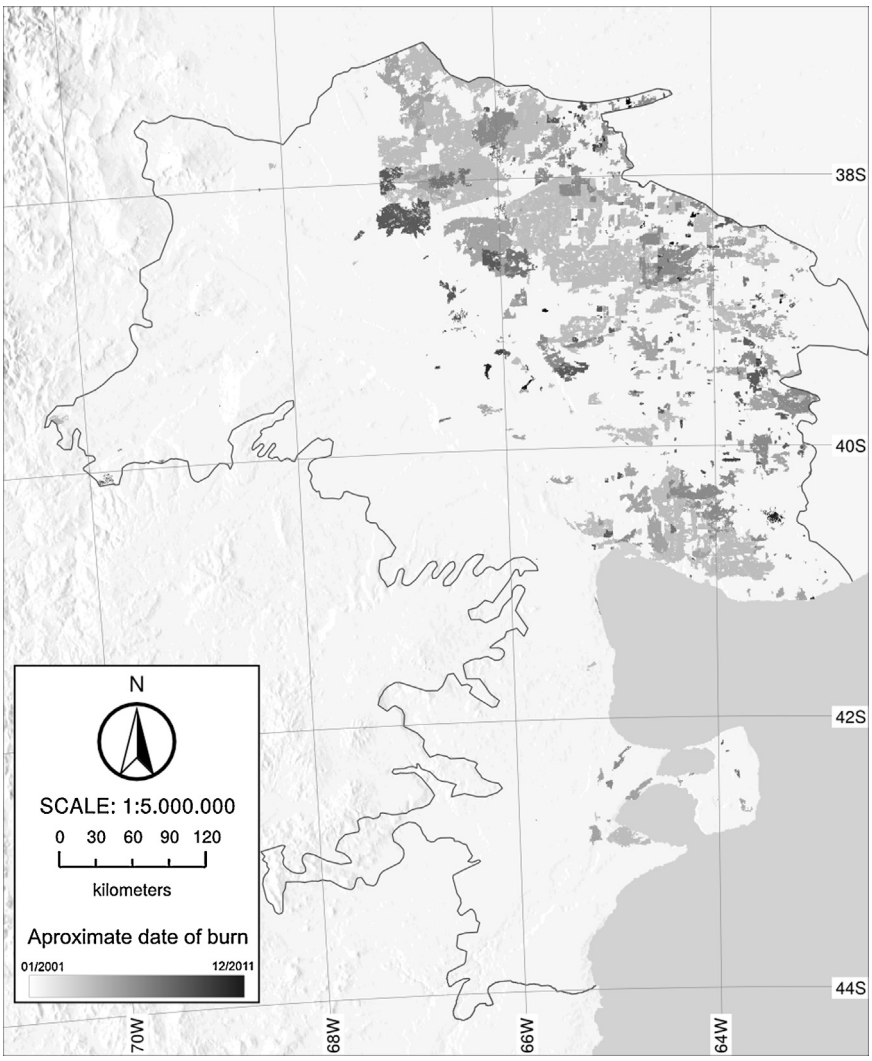

Fig. 10. Burned areas mapped by the burned area algorithm over the 2001–2011 period.

Hawbaker et al. (2008) found 82% of agreement between MOD14A2 and reference data, with detection rates decreasing with fire size. Furthermore, they pointed out that some large fires (over 2000 ha) occurring on shrubland were not detected. The authors argue that it may be due to the darkening of the sensors because of the smoke in the fire front, or a relatively low fuel load causing that once the fire front passes, the burned area no longer emits enough energy to be detected. This is particularly relevant in our area due to the similarity in vegetation cover type.

Comparing MOD14A2 with MOD45A1 Roy et al. (2008) found the active fire product detected larger burned areas than the MODIS burned area product, in concordance with our results. Furthermore, Roy and Boschetti (2009) compared SPOT VEGETATION L3JRC with MOD45A1 and found that the former underestimated much of the burned area (only detected 14%), unlike our results; while MOD45A1 moderately underestimated burned areas (75%, similar to our results). The authors argued that global burned area products fail to meet accuracy requirements for local or regional scale mapping.

These findings highlight that algorithm accuracy is dependent on ecosystem type and size of burned areas to be detected; thus the algorithms should be designed and validated considering the type of coverage, and accounting for inter-seasonal variations to capture a greater variability of fire size.

Table 4
Examples of global fire products validation and accuracy results.

Validated products	Reference data	Geographic region	Accuracy	Reference
MCD45A1 and the backup MODIS burned area product (BMBAP)	Landsat burned-area	South Africa	R^2:0.38–0.86 (MCD45A1), 0.49–0.88 (BMBAP), depending on the vegetation type.	Tsela et al. (2010)
MOD14A1 and MYD14A1	Landsat burned-area	United States	Accuracy values: 73% (MYD14A1), 66% (MOD14A1).	Hawbaker et al. (2008)
MCD45A1, MCD64A1, and a merged product	Landsat burned-area	South Africa	Detection probabilities: 3.0–37.9% (MCD45A1, fractions ≤50%), 12.0–89.2% (MCD64A1, fractions >50%)	Roy et al. (2008)
L3JRC, GlobCarbon, and MOD45A1	Landsat burned-area	Southern Africa	Accuracy values: 14% (L3JRC), 60% (GlobCarbon), 75% (MOD45A1)	Roy and Boschetti (2009)

Spatial-temporal attributes of burned areas

The burned area algorithm allowed us to detect 768 wildfires during the 11 years analyzed (see Fig. 10). The total burned area was computed as 47,330 km^2, which represents 23.11% of the study region. Most of the burned area was burnt by a few large fires; 95% of the burned area (44,960 km^2) was caused by only 18% of the fires. Moreover, the 11 biggest fires burned almost 50% of the total burned area. These large fires mostly occurred in the 2000/2001 season that was particularly dry in the region. On the other hand, fires with sizes smaller than 100 km^2 occurred with higher frequency, about 45 annually. Although they represent about 80% of the fire numbers, they accounted for only 20% of the burned area.

Regarding wildfires recurrence, the analysis indicates that most of the burned areas were burned once over the 11 year period considered in this research, and only 3813 km^2 (or 1.57% of the total area) burned twice. Furthermore only 160 km^2 (or 0.5% of the total burned area) burned three times. The mean fire return interval (analyzed years/total burned area/total area) was of 50.84 years. Even though given the typical life cycles of the vegetation, is near to the expected range for shrublands (20–50 years) to be resilient to wildfires (Keeley, 1986); compared with other studies in similar areas, we found a slightly longer FRI. For example, Stein et al. (2013) found a FRI of less than 35 years and Keeley (2005) found a FRI between 10 and 20 years. These differences could be due to the lesser influence of anthropogenic activities in our region.

If the global products analyzed were used to estimate burned areas, they would lead to significant errors. Taking the burned area algorithm outputs as reference (which would be valid as they showed very good agreement with independent reference data on the validation area), we found that the two MODIS fire products underestimated burned area, mapping only 73% of the burned areas in case of MCD45A1, and 50% in case of MOD14A2 product, while L3JRC greatly overestimate the burned area by 254%.

Conclusions

The semi-desert biome is widely distributed on the earth's surface; the Köpens climate classification places estimates it covers a tenth of the land surface (11.17%). The influence of climate change on wildfires on this type of biome is difficult to predict; although some authors have suggested that an increase of wildfires is very likely to occur directly, due to an increase in climate variability and as a consequence of warmer weather (IPCC, 1996), and indirectly because fires may reduce local precipitation because fire-emitted aerosols increase in the number of cloud condensation nuclei, producing smaller cloud droplets that are less likely to fall as rain (IPCC, 1996). The latter predictions add significance to evaluation studies as discussed in this paper. While global fire products MCD45A1, MOD14A2 and L3JRC appear to deliver well results in ecosystems at global scale, our research demonstrates significant limitations in their ability to detect and map wildfires in semi-arid ecosystems. The global fire related products did not show a good agreement with reference data, which highlights the need for caution when applying these global products at local or regional levels.

The locally-adaptive algorithm we developed using time series of MODIS-derived NBR index outperformed all the global products in mapping the extent and number of burned areas in a semi-arid ecosystems at regional scale. The validation by linear regressions between high resolution data and the burned area algorithm outputs, generated for 11 years of data, indicates that the algorithm accurately maps burned areas (The burned area algorithm validation Section). The developed algorithm is an improvement on previous methods, mainly due to the possibility of keeping relatively relaxed thresholds without compromising commission errors. Since our algorithm uses freely accessible Terra and Aqua MODIS products, it can provide inexpensive, more reliable and salient information for decision-making on land management in semi-arid environments (e.g., shrublands and rangelands). Our findings have significant implications for the implementation of reliable early warning monitoring systems at regional, sub-regional and national scales. Even though we consider that due to its relative simplicity (e.g., few parameters) the algorithm might be easily adapted to other biomes, further research is needed to test its performance in other biomes and to evaluate its accuracy depending on vegetation cover type. In this regard, we are currently working on implementing the burned area algorithm in southern South America, over the 2000–2012 time period.

Our investigation suggest that for detecting burned areas in other geographic regions using this algorithm the following steps are needed prior to implementation: (1) determine the relative inaccuracy of fire detection due to sensor properties (e.g., signal to noise ratio) and scene variability, (2) adjust the algorithm with regard to the NBR thresholds, (3) investigate the sensitivity of semi-automated burned area detection to land cover and its properties, the size and shape of burned areas, and confusion with other forms of vegetation removal. Lastly, fire detection algorithms can improve detection accuracy if the user community plays an active role in defining fire product requirements, becoming actively involved in product development, implementation, and validation efforts.

References

Archibald, S., Roy, D., van Wilgen, B., Scholes, R., 2008. What limits fire? An examination of drivers of burnt area in Southern Africa. Global Change Biol. 15, 613–630.

Ares, J., Beeskow, A., Bertiller, M., Rostagno, M., Irisarri, M., Anchorena, J., Merino, C., 1990. Structural and dynamic characteristics of overgrazed lands of Northern Patagonia, Argentina Ecosystems of the World 17A, 149–175.

Barbosa, P., Cardoso Pereira, J., Grégoire, J.-M., 1998. Compositing criteria for burned area assessment using multitemporal low resolution satellite data. Remote Sens. Environ. 65, 38–49.

Boschetti, L., Brivio, P., Eva, H., Gallego, J., Baraldi, A., Grégoire, J., 2006. A sampling method for the retrospective validation of global burned area products. Geosci. Remote Sens. 44, 1765–1773.

Bruzzone, L., Prieto, D., 2002. An adaptive semiparametric and context-based approach to unsupervised change detection in multitemporal remote-sensing images. IEEE Trans. Image Process. 11, 452–466.

Chuvieco, E., Englefield, P., Trishchenko, A., Luo, Y., 2008. Generation of long time series of burn area maps of the boreal forest from NOAA AVHRR composite data. Remote Sens. Environ. 112, 2381–2396.

Chuvieco, E., Kasischke, E., 2007. Remote sensing information for fire management and fire effects assessment. J. Geophys. Res. Biogeosci. 112, 1–8.

Claraz, G., 1988. Diario de viaje de exploración al Chubut. Buenos Aires, Marymar. 189, 1865–1866.

De Klerk, H., 2008. A pragmatic assessment of the usefulness of the MODIS (Terra and Aqua) 1-km active fire (MOD14A2 and MYD14A2) products for mapping fires in the fynbos biome. Int. J. Wildland Fire 17, 166–178.

Defosse, G., Rostagno, C., del Valle, H., Dentoni, M., 2003. El fuego en la porción austral de la región del Monte. In: Kunst, C., Bravo, S., Panigatti, J. (Eds.), Fuego en los Ecosistemas Argentinos. INTA, Buenos Aires, pp. 167–180.

del Valle, H., Novara, M., Rostagno, M., Defossé, G., Coronato, F., 2004. Cartografía de Areas Quemadas con Sensores Remotos Opticos y de Radar en Ecosistemas Secos del Noreste de Patagonia Central. In: Navone, S., Rosatto, H., Vilella, F. (Eds.). Teledetección Aplicada a la Problemática Ambiental Argentina, Buenos Aires: FAUBA, pp. 1–16.

Escuin, S., Navarro, R., Fernández, P., 2008. Fire severity assessment by using NBR (normalized burn ratio) and NDVI (normalized difference vegetation index) derived from LANDSAT TM/ETM images. Int. J. Remote Sens. 29, 1053–1073.

Eva, H., Lambin, E., 1998. Remote sensing of biomass burning in tropical regions: sampling issues and multisensor approach. Remote Sens. Environ. 64, 292–315.

Fernandez, A., Illera, P., Casanova, J., 1997. Automatic mapping of surfaces affected by forest fires in Spain using AVHRR NDVI composite image data. Remote Sens. Environ. 60, 153–162.

Flannigan, M., Stocks, B., Turetsky, M., Wotton, M., 2009. Impacts of climate change on fire activity and fire management in the circumboreal forest. Global Change Biol. 15, 549–560.

Forsyth, G., Van Wilgen, B., 1998. The recent fire history of the Table Mountain National Park and implications for fire management. Afr. Prot. Area Conserv. Sci. 50, 3–9.

Fraser, R., Li, Z., Cihlar, J., 2000. Hotspot and NDVI differencing synergy (HANDS): a new technique for burned area mapping over Boreal forest. Remote Sens. Environ. 74, 362–376.

Garcia, M., Chuvieco, E., 2004. Assessment of the potential of SAC-C/MMRS imagery for mapping burned areas in Spain. Remote Sens. Environ. 92, 414–423.
Giglio, L., Loboda, T., Roy, D., Quayle, B., Justice, C., 2009. An active-fire based burned area mapping algorithm for the MODIS sensor. Remote Sens. Environ. 113, 408–420.
Giglio, L., van der Werf, G., Randerson, J., Collatz, G., Kasibhatla, P., 2006. Global estimation of burned area using MODIS active fire observations. Atmos. Chem. Phys. 6, 957–974.
Gómez, I., Martín, M., 2011. Prototyping an artificial neural network for burned area mapping on a regional scale in Mediterranean areas using MODIS images. Int. J. Appl. Earth Obs. Geoinf. 13, 741–752.
Grégoire, J., Tansey, K., Silva, J., 2003. The GBA2000 initiative: developing a global burnt area database from SPOT-VEGETATION imagery. Int. J. Remote Sens. 24, 1369–1376.
Hawbaker, T., Radeloff, V., Syphard, A., Zhu, Z., Stewart, S., 2008. Detection rates of the MODIS active fire product in the United States. Remote Sens. Environ. 112, 2656–2664.
Hijmans, R., Cameron, S., Parra, J., Jones, P., Jarvis, A., 2005. Very high resolution interpolated climate surfaces for global land areas. Int. J. Climatol. 25, 1965–1978.
IPCC, 1996. Impacts, Adaptation and Mitigation Options. IPCC, Working Group II, Cambridge. Cambridge University Press, pp. 878.
Justice, C., Giglio, L., Korontzi, S., Owens, J., Morisette, J., Roy, D., Kaufman, Y., 2002. The MODIS fire products. Remote Sens. Environ. 83, 244–262.
Keeley, J., 1986. Resilience in mediterranean-type ecosystems. In: Dell, B., Hopkins, A., Lamont, B. (Eds.), Tasks for Vegetation Science. Springer, Dordrecht, Netherlands, pp. 95–112.
Keeley, J., 2005. Fire history of the San Francisco East Bay region and implications for landscape patterns. Int. J. Wildland Fire 14, 285–296.
Keeley, J., 2009. Fire intensity, fire severity and burn severity: a brief review and suggested usage. Int. J. Wildland Fire 18, 116–126.
Keeley, J., Brennan, T., Pfaff, A., 2008. Fire severity and ecosytem responses following crown fires in california shrublands. Ecol. Appl. 18, 1530–1546.
Key, C., Benson, N., 1999. Measuring and remote sensing of burn severity: the CBI and NBR. Poster abstract. In: Neuenschwander, L., Ryan, K., Goldberg, G. (Eds.), Proceedings of the Joint Fire Science Conference, Vol. II, Boise, ID, 15-17 June 1999. University of Idaho and International Association of Wildland Fire, p. 284.
Key, C., Benson, N., 2006. Landscape assessment: ground measure of severity, the composite burn index; and remote sensing of severity, the normalized burn ratio. In: Lutes, D., Keane, R., Caratti, J., Key Benson, C.N., Sutherland, S., Gangi, L. (Eds.), FIREMON: Fire Effects Monitoring and Inventory System. USDA Forest Service, Rocky Mountain Research Station, Ogden, UT, UT. Gen. Tech. Rep. RMRS-GTR-164-CD: LA.
Labraga, J., Villalba, R., 2009. Climate in the monte desert: past trends, present conditions, and future projections. J. Arid Environ. 73, 154–163.
Lanorte, A., Danese, M., Lasaponara, R., Murgante, B., 2011. Multiscale mapping of burn area and severity using multisensor satellite data and spatial autocorrelation analysis. Int. J. Appl. Earth Observ. Geoinform. 20, 42–51.
León, R., Bran, D., Collantes, M., Paruelo, J., Soriano, A., 1998. Grandes unidades de vegetación de la Patagonia extra andina. Ecología Austral 8, 125–144.
Libonati, R., DaCamara, C., Pereira, J., Peres, L., 2010. Retrieving middle-infrared reflectance for burned area mapping in tropical environments using MODIS. Remote Sens. Environ. 114, 831–843.
Loboda, T., O'Neal, K., Csiszar, I., 2007. Regionally adaptable *d*NBR-based algorithm for burned area mapping from MODIS data. Remote Sens. Environ. 109, 429–442.
Maier, S., 2010. Changes in surface reflectance from wildfires on the Australian continent measured by MODIS. Int. J. Remote Sens. 31, 3161–3176.
Maier, S., Russell-Smith, J., Edwards, A., Yates, C., 2013. Sensitivity of the MODIS fire detection algorithm (MOD14) in the savanna region of the Northern Territory, Australia. ISPRS J. Photogramm. Remote Sens. 76, 11–16.
Martín, M., Gómez, I., Chuvieco, E., 2006. Burnt area index (BAIM) for burned area discrimination at regional scale using MODIS data. For. Ecol. Manage. 234S, S221.
Mitri, G., Gitas, I., 2002. The development of an object-oriented classification model for operational burned area mapping on the Mediterranean island of Thasos using LANDSAT TM images. In: Viegas, D. (Ed.), IV International Conference on Forest Fire Research & Wildland Fire Safety. Rotterdam Millpress, p. 79.
Pratt, W.K., 2001. Digital Image Processing. NY: Wiley-Interscience, New York, pp. 491–556.
Quintano, C., Fernández-Manso, A., Stein, A., Bijker, W., 2011. Estimation of area burned by forest fires in Mediterranean countries: a remote sensing data mining perspective. For. Ecol. Manage. 262, 1597–1607.
Rollins, M., Keane, R., Parsons, R., 2004. Mapping fuels and fire regimes using remote sensing, ecosystem simulation, and gradient modeling. Ecol. Appl. 14, 75–95.
Roy, D., Boschetti, L., 2009. Southern Africa validation of the MODIS, L3JRC, and GlobCarbon burned-area products. IEEE Trans. Geosci. Remote Sens. 47, 1032–1044.
Roy, D., Boschetti, L., Justice, C., Ju, J., 2008. The collection 5 MODIS burned area product – global evaluation by comparison with the MODIS active fire product. Remote Sens. Environ. 112, 3690–3707.
Roy, D., Jin, Y., Lewis, P., Justice, C., 2005. Prototyping a global algorithm for systematic fire-affected area mapping using MODIS time series data. Remote Sens. Environ. 97, 137–162.
Roy, D., Lewis, P., Justice, C., 2002. Burned area mapping using multi-temporal moderate spatial resolution data-a bi-directional reflectance model-based expectation approach. Remote Sens. Environ. 83, 264–287.
Siljeström, R., Moreno-Lopez, A., 1995. Monitoring burnt areas by principal components analysis of multi-temporal TM data. Int. J. Remote Sens. 16, 1577–1587.
Silva, J., Sá, A., Pereira, J., 2005. Comparison of burned area estimates derived from SPOT-VEGETATION and Landsat ETM+ data in Africa: influence of spatial pattern and vegetation type. Remote Sens. Environ. 96, 188–201.
Simon, M., Plummer, S., Fierens, F., Hoelzemann, J., Arino, O., 2004. Burnt area detection at global scale using ATSR-2: the GLOBSCAR products and their qualification. J. Geophys. Res. 109, 1–18.
Soriano, A., Movia, C., Leon, R., 1983. Vegetation. In Deserts and semi-deserts of Patagonia. Elsevier, Amsterdam, pp. 440–454.
Stein, S.M., Menakis, J., Carr, M.A., Comas, S., Stewart, S.I., 2013. Wildfire, Wildlands, and People: Understanding and Preparing for Wildfire in the Wildland-Urban Interface. Fort Collins, CO., U.S, pp. 36.
Tansey, K., Beston, J., Hoscilo, A., Page, S., Paredes Hernández, C., 2008a. Relationship between MODIS fire hot spot count and burned area in a degraded tropical peat swamp forest in Central Kalimantan. Indonesia. J. Geophys. Res. 113, D23112.
Tansey, K., Grégoire, J.-M., Defourny, P., Leigh, R., Pekel, J.-F., van Bogaert, E., Bartholomé, E., 2008b. A new, global, multi-annual (2000–2007) burnt area product at 1 km resolution. Geophys. Res. Lett. 35, 1–6.
Thonicke, K., Venevsky, S., Sitch, S., Cramer, W., 2001. The role of fire disturbance for global vegetation dynamics: coupling fire into a dynamic global vegetation model. Global Ecol. Biogeogr. 10, 661–677.
Tsela, P., van Helden Frost, P., Wessels, P., Archibald, K.S., 2010. Validation of the MODIS burned-area products across different biomes in South Africa. In: IEEE International Geoscience and Remote Sensing Symposium (IGARSS), Honolulu, Hawaii, USA July 25–30.
Tsela, P., Wessels, K., Botai, J., Archibald, S., Swanepoel, D., Steenkamp, K., Frost, P., 2014. Validation of the two standard MODIS satellite burned-area products and an empirically-derived merged product in South Africa. Remote Sens. 6, 1275–1293.
Villagra, P., Defosse, G., del Valle, H., Tabeni, S., Rostagno, C., Cesca, E., Abraham, E., 2009. Land use and disturbance effects on the dynamics of natural ecosystems of the Monte Desert: implications for their management. J. Arid Environ. 73, 202–211.
Williamson, G., Price, O., Henderson, S., Bowman, D., 2013. Satellite-based comparison of fire intensity and smoke plumes from prescribed fires and wildfires in south-eastern Australia. Int. J. Wildland Fire 22, 121–129.